ELSEVIER

Journal of Power Sources 94 (2001) 1–8

JOURNAL OF POWER SOURCES

www.elsevier.com/locate/jpowsour

The origin of capacity loss in the pocket plate cadmium electrode

Nina Simic[a], Rune Sjövall[b], Ulrik Palmqvist[c], Elisabet Ahlberg[a,*]

[a]*Department of Chemistry, Göteborg University, S-412 96 Göteborg, Sweden*
[b]*SAFT AB, Box 709, S-572 28 Oskarshamn, Sweden*
[c]*Arrhenius Laboratories, Stockholm University, S-106 91 Stockholm, Sweden*

Received 3 January 2000; received in revised form 30 July 2000; accepted 4 September 2000

Abstract

Electrical testing of negative limited mono-pocket plate cells, cyclic voltammetry and surface analysis by X-ray diffraction were used to investigate the origin of the second discharge plateau at the cadmium pocket plate electrode. The electrical testing results show that there is a direct coupling between the appearance of a second discharge plateau and a high carbonate concentration in combination with high discharge rates (1 C_5A). An exchange to a carbonate free electrolyte results in recovering of the cell. Voltammetric measurements show that the reduction of $CdCO_3$ takes place in the same potential region as the reduction of $Cd(OH)_2$. Thus, the presence of $CdCO_3$ in the discharged negative electrode cannot give rise to a second voltage plateau or capacity loss. However, a decrease in the hydroxide concentration results in a positive shift of the oxidation potential. These results are interpreted in the context of the porous structure of the pocket plate cadmium electrode. For a high carbonate concentration and large discharge rates, the hydroxide concentration within the pores are depleted leading to a positive potential shift and the appearance of a second discharge plateau.

Keywords: Nickel–cadmium battery; Cadmium electrode; Cyclic voltammetry; X-ray diffraction; Second discharge plateau

1. Introduction

In order to understand the behaviour of the Ni–Cd battery during operation, several investigations have been performed during the years, both of more fundamental electrochemical character and as applied battery studies. Despite this, there are still unanswered questions about the Ni–Cd battery performance during use. Below a short description of the fundamental electrochemistry of the cadmium electrode is described as well as applied battery problems such as ageing and memory effects. This paper deals with the second discharge plateau occurring in the discharge curve of the cadmium electrode. The investigation concerns the pocket plate Cd-electrode and contains electrochemical studies of the active battery material.

From a fundamental point of view, the oxidation mechanism of the cadmium electrode is generally assumed to involve dissolved intermediates [1–6]. Most studies of the electrochemical mechanism have been performed at planar or amalgamated electrodes. The electrochemical characteristics of porous cadmium electrodes have also been the subject of a large number of investigations and documented under a variety of conditions [7–14]. Studies of porous cadmium electrodes are less well understood because of complications such as mass transfer limitations, unknown electrolyte concentration within the pores, agglomeration (increase in particle size) of cadmium hydroxide, etc. The fundamental studies of the cadmium electrode together with the studies of a more applied approach have lead to a better understanding of the system. Below, the general ageing and the memory effect of the battery electrode is described.

1.1. Ageing of the cadmium electrode

Several phenomena are thought to cause electrode failure in the cadmium electrode, such as crystal growth, redistribution of active material, pore blocking, formation of passivating film, etc. [15–18]. Passivation and agglomeration due to precipitation and electrodeposition of dissolved cadmium species were found to cause significant loss in electrode capacity on repeated charge and discharge [19]. The particle size was found to increase with an increasing number of cycles and decreasing charge rate [17]. As a consequence of this agglomeration, a mass transfer problem within the hydroxide appears, whereby the inner parts of the electrode cease to participate in the discharge reaction. Scanning electron microscopy and optical studies show that

* Corresponding author. Tel.: +46-31-772-2879; fax: +46-31-772-2853.
E-mail address: ela@inoc.chalmers.se (E. Ahlberg).

0378-7753/01/$ – see front matter
PII: S0378-7753(00)00596-6

cadmium metal deposition could take place on top of cadmium hydroxide or oxide crystallites [7,8]. This process was proposed to be a possible mechanism of occlusion of active material. This is in contrast to the results presented recently where reduction of cadmium hydroxide was shown to be highly facilitated at cadmium metal compared to other conducting substrates [3,4]. However, after extended cycling parts of the active material indeed cease to participate in the cycling and the unchargeable cadmium hydroxide phase has been reported as inactive [17,20], although only β- and γ-$Cd(OH)_2$ can be detected on the negative material. In a recent discharge study [3,4], it was clearly shown that the reduction of γ-$Cd(OH)_2$ and in particular β-$Cd(OH)_2$ takes place at large overpotentials in the absence of cadmium metal support. Thus, the inactive phase of cadmium hydroxide reported in the literature is probably not in direct contact with cadmium metal and therefore requires high overpotentials to get reduced [3].

Another issue with the Ni–Cd battery is the carbonation of the electrolyte. During operation, the carbonate concentration of the battery electrolyte increases, due to graphite oxidation and absorption of CO_2 from the air. At increased carbonate concentrations in the cell, the negative electrode loses capacity [21]. Other studies have reported cadmium carbonates as a product during anodic oxidation of cadmium in carbonate containing electrolytes [22,23]. Both carbon dioxide contamination from the air and graphite oxidation in the electrodes convert carbon into CO_3^{2-} through the consumption of hydroxide ions [24,25]. As the hydroxide ions are consumed the electrolyte resistance is increased in the battery cell, resulting in decreased capacity. Experiments have shown that if the carbonate concentration is increased but the hydroxide concentration is kept constant, the capacity loss is not as severe as in the case where hydroxide ions are consumed [24].

1.2. Memory effect

Memory effect is the name given to the phenomenon whereby a Ni–Cd battery loses the ability to deliver full capacity, after having been partially utilised over a prolonged period of time. Apart from irreversible deterioration this is a temporary effect that can be erased by complete discharging followed by rapid charging. The mechanisms behind this are not fully understood but one explanation has been that the unused portion of the charged negative active material undergoes a morphological change which makes it difficult to discharge [16,18,26].

Alloy formation is another phenomenon that results in an erasable capacity loss. It appears after the battery has been subjected to high temperature overcharge and is caused by the formation of Ni–Cd intermetallic phases such as Ni_2Cd_5 and Ni_5Cd_{21}. The intermetallic phases have an approximately 100–120 mV more positive discharge potential than the cadmium electrode. When parts of the cadmium are bound to the intermetallic phases there is a voltage step of about 100–120 mV in the discharge curve. The amount of intermetallic phases increases with overcharge time and consequently the capacity gradually decreases. This effect can be erased by complete discharge and subsequent charging, during which pure cadmium is re-formed. The alloy formation can be prevented by not using nickel as a conducting aid in the negative electrode [16,18,26,27].

Laboratory tests of Ni–Cd pocket plate batteries subjected to constant voltage charging showed that a second voltage plateau can appear at the positive electrode. The plateau is believed to appear whenever increased internal resistance arises within the electrode, whether due to graphite loss, swelling or some other factor [25]. In some cases, the second voltage plateau appeared at the cadmium electrode at high discharge rates and high carbonation of the electrolyte. The present investigation concerns the second voltage plateau caused by the negative electrode.

2. Experimental

2.1. Electrode material

A conventional composition of the negative electrode active material was used in this investigation, with β-$Cd(OH)_2$ as the main component and with additions of iron oxide and graphite. The active material was exposed to cycling in mono-pocket plate cells. The electrochemical properties of the active material were investigated with the aid of the carbon paste electroactive electrode technique in a conventional three-electrode cell.

2.2. Electrolyte description

2.2.1. Mono-pocket plate cell

Two different electrolytes, one fresh lithiated (E1) and one from an old battery cell (E2), were used for the mono-pocket cell experiments (Table 1). E2 was taken from a cell that had been subjected to constant voltage charging at room temperature for more than 2 years. Consequently, this electrolyte exhibited a higher degree of carbonation than the fresh one. Electrolyte analyses were also carried out during the mono-pocket plate experiments since composition changed due to the test programme and the handling of the cell (Table 1).

2.2.2. Voltammetric experiments

Three different battery type electrolytes (E3, E4 and E5) were used in the voltammetric experiments. In contrast to the mono-pocket plate experiments, the electrolyte compositions are not changed during the voltammetry due to the large volume of electrolyte and the small amount of active material. Therefore, only the initial compositions are presented in Table 2.

For the pH dependence experiments, 1 and 0.1 M KOH (referred to as pH 14 and 13, respectively) was prepared

Table 1
Analysis of electrolyte composition

Type of electrolyte	Sample (fresh)	Sample (from old cell)	
	A1/A2 (M)	B1 (M)	B2 (M)
Starting electrolyte:	E1	E2	E2
KOH	5.2	2.5	2.5
K_2CO_3	0.03	0.9	0.9
LiOH	0.5	0.5	0.5
Prior to 1st electrolyte exchange of B2:			
KOH	5.4[a]	2.7[a]	2.6[a]
K_2CO_3	0.05	1.0	1.0
LiOH	0.5	0.5	0.5
Prior to 2nd electrolyte exchange of B2:			
KOH	5.4	2.7	4.3
K_2CO_3	0.07	1.0	0.08
LiOH	0.6	0.5	0.06[b]
After final test:			
KOH	Not analyzed	2.6	5.2
K_2CO_3		1.0	0.05
LiOH		0.5	0.6

[a] Increase in the hydroxide concentration due to water loss.
[b] The electrolyte was not lithiated in this exchange.

Table 2
Analysis of electrolyte composition

Electrolyte	E3 (fresh) (M)	E4 (from old cell) (M)	E5 (from old cell) (M)
KOH	5.1	3.4	0.9
K_2CO_3	0.009	0.3	1.3
LiOH	0.6	0.4	0.4

from supra pure $KOH{\cdot}H_2O$ from Merck and Co., Inc. and doubly distilled, deaerated and decarbonated water. Appropriate mixtures of K_2CO_3 and $KHCO_3$ were dissolved in doubly distilled, deaerated and decarbonated water in order to achieve alkaline solutions of pH 10, 11 and 12 with an ionic strength of 0.1 M, and no additional ions except for the carbonate system. The amounts of K_2CO_3 and $KHCO_3$ were calculated using the pK_a and the desired hydroxide ion concentrations, where the pK_a used was 10.01 [28].

2.2.3. Electrical testing of mono-pocket plate cells

The negative electrodes were made by pressing briquettes of the active material with dimensions 60 mm × 12 mm × 1.6 mm (weighing about 3.2 g). The briquette was encapsulated between two perforated nickel-plated steel strips, forming a mono-pocket. This pocket was in turn welded to a nickel-plated steel lug. The capacity was 260 mAh per gram active material. The positive and reference electrodes consisted of a nickel sheet and a zinc rod, respectively. This cell construction results in measuring only the capacity of the negative electrode. Both E1 and E2 were used in the tests. The electrolyte volume in each cell was about 400 ml. The cells were filled up with deionized water to compensate for water loss during testing. The electrode capacity measurements were performed at a discharge rate of 0.2 C_5A and 1.0 C_5A to 0.8 V versus a Zn/ZnO reference electrode, $E = -1.3$ V versus SHE. Charging was performed at 0.2 C_5A. In Table 3, a summary of the test procedure is shown. After the electrical testing, the electrode active material used for the X-ray analyses was dismantled followed by thorough washing with deionized water until the pH of the filtrate was in the range 9–10.

2.3. Electrochemical experiments

For the more fundamental experiments, a conventional three-electrode cell was used with platinum gauze as the auxiliary electrode. The potential was measured against a saturated potassium chloride calomel electrode, $E = 241.5$ mV with respect to SHE. All experiments were carried out at room temperature. The electrolyte was purged with highly purified nitrogen for at least 30 min before the

Table 3
Scheme for the mono-pocket testing

1.	Fill-up with lithiated electrolyte (20 g LiOH/l) for samples A1 and A2, and with electrolyte from an old cell for samples B1 and B2.
2.	Electrolyte analysis.
3.	Leaching at room temperature (RT) for 8 h.
4.	Two cycles of formation at rate of charge 0.2 C_5A for 8 h and at discharge 0.2 C_5A for 5 h.
5.	Capacity determination after charging at rate 0.2 C_5A for 8 h and discharging at 0.2 C_5A to end voltage 0.8 V versus zinc/zinc oxide.
6.	Capacity determination after charging at rate 0.2 C_5A for 8 h and discharging at 1.0 C_5A to end voltage 1.0 V versus zinc/zinc oxide.
7.	Increase of temperature to 50°C.
8.	Capacity determination after charging at rate 0.2 C_5A for 8 h and discharging at 0.2 C_5A to end voltage 0.8 V versus zinc/zinc oxide.
9.	Capacity determination after charging at rate 0.2 C_5A for 8 h and discharging at 1.0 C_5A to end voltage 1.0 V versus zinc/zinc oxide.
10.	Electrolyte analysis.
11.	Change to fresh electrolyte (without LiOH) for sample B2.
12.	"Ageing" test at rate of charge 1.0 C_5A for 8 h followed by discharge at 1.0 C_5A to end voltage 1.0 V versus zinc/zinc oxide.
13	Electrolyte analysis.
14.	Change to fresh lithiated (13 g LiOH/l) electrolyte for sample B2.
15.	Capacity determination after charging at rate 0.2 C_5A for 8 h and discharging at 0.2 C_5A to end voltage 0.8 V versus zinc/zinc oxide.
16.	Capacity determination after charging at rate 0.2 C_5A for 8 h and discharging at 1.0 C_5A to end voltage 1.0 V versus zinc/zinc oxide.
17.	Electrolyte analysis.

experiment was started and a flow of nitrogen gas was maintained above the solution during the experiment to prevent oxygen contamination. An EG&G Princeton Applied Research Potentiostat/Galvanostat, Model 273A, was used.

2.3.1. Preparation of the carbon paste electrode

The carbon paste electroactive electrode (CPEE) consisted of commercial carbon paste with a non-conducting binder (Metrohm) and finely grained samples. The carbon paste and the sample were thoroughly mixed together in a mortar in order to obtain a homogeneous paste. The electroactive paste was placed as an approximately 1.5 mm thick layer over a carbon paste layer, which had previously been pressed into an epoxy cavity. This was done in order to ensure adhesion between the electroactive paste and the rest of the electrical connections in the electrode. The surface of the electrode was smoothed with a spatula and excess paste was removed with a sharp steel blade. Electrical connection to the graphite paste was made by plugging a platinum wire at the bottom of the cavity into a brass rod. The electrode surface area was 0.2 cm^2. The mixing ratios, by weight, were *E*:CP (Electroactive material:Carbon paste) = 1:6 for all materials. The *E*:CP ratio were optimised for physical stability and current response. The carbon paste electrode technique has recently been used in fundamental studies of the cadmium electrode [3,4].

2.4. Chemical and surface analyses

2.4.1. Chemical

The concentrations of carbonate, hydroxide and lithium ions in the electrolyte were determined by ordinary acid–base titration and by atomic absorption spectrometer measurements (Varian; AA-1275).

2.4.2. X-ray diffraction (XRD)

XRD analyses were performed on a Philips PW3050 diffractometer utilizing Co Kα radiation. The measurements were made at 0.030° intervals of 2θ over the range 5–80° using a count-time of 1 s for each step.

3. Results and discussion

3.1. Lab cell with mono-pocket plate electrodes

In order to avoid the influence of the battery cell design, laboratory cell experiments were performed on mono-pocket plate negative and nickel sheet positive electrode with electrolyte in excess. The reactions occurring at the nickel sheet were oxygen evolution during charging and hydrogen evolution during discharging respectively, and consequently the cells were negatively limited. In two cells (A1 and A2) electrolyte with low initial carbonate concentration (0.03 M) was used and in another two cells (B1 and B2) electrolyte with high initial carbonate concentration (0.9 M) was used. The compositions of the electrolytes are shown in Table 1.

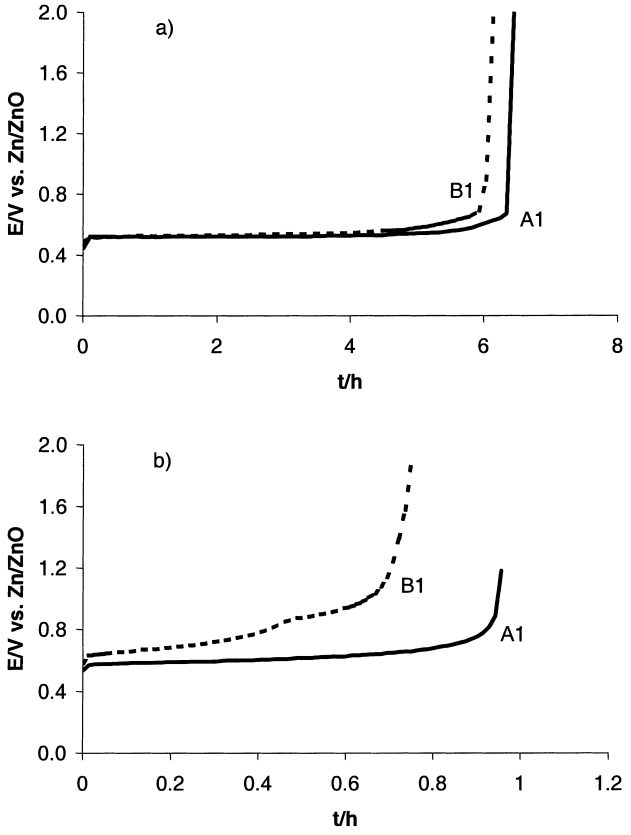

Fig. 1. Discharge curves at (a) 0.2 C_5A (Table 3 point 5); and (b) 1 C_5A (Table 3 point 6) at room temperature.

The whole procedure for the pocket plate testing is presented in Table 3. After the formation and charging, the electrodes were discharged at 0.2 C_5A to a potential of 0.8 V versus Zn/ZnO at room temperature (point 1–5 in Table 3), Fig. 1a. The discharge curves for A1 and B1 are shown in Figs. 1a, 1b, 2a and b, the discharge curves for A2 and B2 are not shown since A1 resemble A2 and B1 resemble B2 in these experiments. No second discharge plateau was present, the only difference between the two electrolytes is a slightly lower capacity (about 8%) for the cells with high carbonate concentration. After re-charging, the same experiment was performed at a discharge rate of 1.0 C_5A (point 6 in Table 3), Fig. 1b. In this experiment, a very clear second discharge plateau appears for cells B1 and B2, which is also accompanied by significant capacity loss. Cells A1 and A2 exhibited normal discharge curves. The appearance of the second discharge plateau is clearly dependent on both the carbonate concentration of the electrolyte and the discharge rate.

The same testing was performed at 50°C in order to simulate extreme operating conditions. The cells were heated up to 50°C and charged/discharged at 0.2 C_5A (point

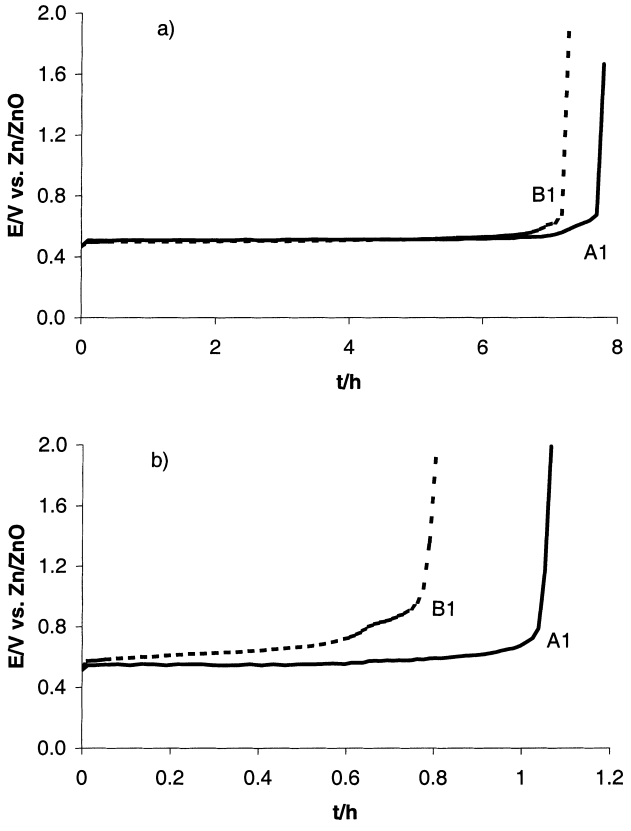

Fig. 2. Discharge curves at (a) 0.2 C_5A (Table 3 point 8); and (b) 1 C_5A (Table 3 point 9) at 50°C.

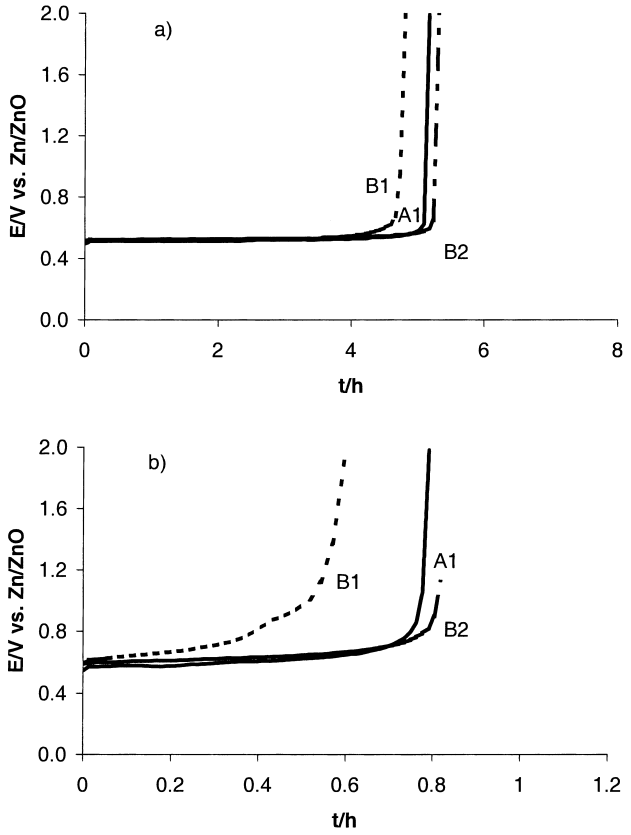

Fig. 3. Discharge curves at (a) 0.2 C_5A (Table 3 point 15); and (b) 1 C_5A (Table 3 point 16) at room temperature. The electrolyte is exchanged in cell B2.

7–9 in Table 3). The same results as at room temperature were obtained, Fig. 2a and b. All capacities were increased during the charge/discharge cycle at 50°C compared to the same discharge rate at room temperature. It is commonly observed that the capacity increases during the first cycles at elevated temperatures and an investigation of this phenomenon is in progress.

The next step was exchange of the electrolyte in cell B2 followed by charging of all four cells at room temperature. After two electrolyte changes, cell B2 exhibited the highest capacity during subsequent discharge at 0.2 C_5A, followed by A1, A2 and B1, respectively (point 10–15 in Table 3). However, B2 did not reach its initial capacity, shown in Fig. 1a, due to common ageing. No cells had a second discharge plateau, Fig. 3a. The cells were then subjected to a discharge rate of 1.0 C_5A (point 16 in Table 3), Fig. 3b. Cell B1, with an electrolyte with high carbonate concentration, still showed the second voltage plateau, while cell B2, with new fresh electrolyte, had the best capacity of all cells and did not have a second discharge plateau, Fig. 3b. Cell B2 is therefore almost completely recovered after electrolyte exchange, the small decrease in capacity is due to common ageing. Cells A1 and A2 still had no second discharge plateau, but a slightly lower capacity than cell B2. This can be explained by increased carbonate concentration in A1 and A2 resulting from the charge/discharge cycling in addition to the common ageing. The appearance of the second discharge plateau is clearly dependent on the carbonate concentration of the electrolyte and the discharge rate.

3.2. Voltammetry

The section above shows that during discharge in electrolytes with high carbonate concentration and high discharge rates a second discharge plateau is formed in the discharge curve for the cadmium electrode. Fundamental studies have shown that during oxidation of cadmium in a carbonate containing electrolyte, $CdCO_3$ can be formed [22,23]. This makes it interesting to study the electrochemical behaviour of $CdCO_3$.

It is also interesting to study the electrochemical behaviour of a planar carbon paste electrode of the active material in order to avoid the mass transfer problem that occurs at a porous electrode. The porous structure of the electrode leads to a mass transfer problem, which results in a depletion of hydroxide ions during discharge (discussed below). In order to simulate this depletion of hydroxide ions, the pH dependence of a planar carbon paste electrode was investigated, i.e. under conditions where the response only represent the redox reaction of the active material.

The reduction of $CdCO_3$ in carbon paste was studied in the different battery electrolytes (E3, E4 and E5) and the

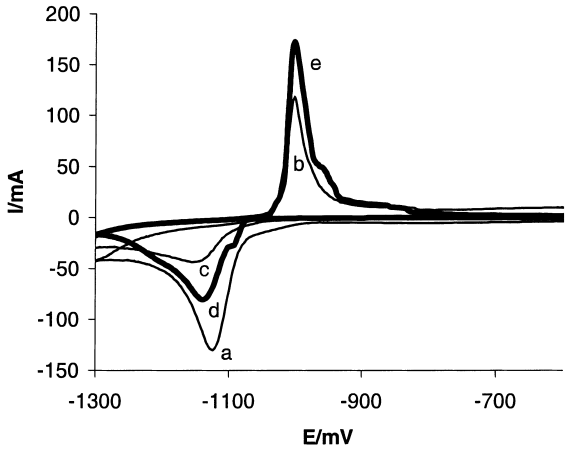

Fig. 4. Cyclic voltammogram of a CPEE with $CdCO_3$ (fine). Peak (a) is the first reduction of $CdCO_3$ to Cd, peak (b) is the following oxidation of Cd and peak (c) is the final reduction of $Cd(OH)_2$. Cyclic voltammogram of a CPEE containing the active material (bold). The scan rate was 1 mV/s and the electrolyte E3.

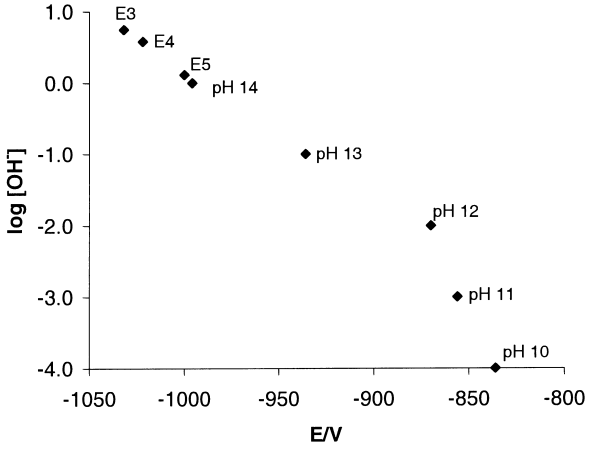

Fig. 5. Electrode potential as a function of hydroxide concentration.

voltammetric response is shown in Fig. 4 for one of the electrolyte compositions (E3). Peak (a) corresponds to the reduction of the carbonate, forming cadmium metal. The electrode was then swept in positive direction and cadmium was oxidised, peak (b). Cadmium hydroxide is the probable product since the hydroxide concentration is high and the carbonate concentration is very low and the voltammogram after the first reduction resembles the cyclic voltammogram of a cadmium metal electrode in 7 M KOH where the product was β-$Cd(OH)_2$, as detected by FTIR (Fourier Transform Infrared Spectroscopy) [4]. The potential was finally swept in negative direction and the hydroxide was then reduced to cadmium metal (c). For comparison, the voltammogram of the active material (described in Section 2.1) is shown in the same figure (bold), where peak (d) corresponds to the reduction of $Cd(OH)_2$ to Cd and peak (e) to the oxidation of Cd to $Cd(OH)_2$. It can be seen that the reduction of $CdCO_3$ is as facile as the reduction of the active material. The same result is obtained in the different electrolytes used in this work. The presence of cadmium carbonate in the discharged negative material will therefore not influence the charging properties of the battery electrode since both cadmium hydroxide and cadmium carbonate will be reduced to cadmium metal as long as the material is in contact with a conductor.

The oxidation behaviour of cadmium in the battery electrolytes (E3, E4 and E5) shows that there is a slight shift (43 mV) of the anodic peak in positive direction as the carbonate concentration is increased (not shown in figure). The increase of carbonate concentration is accompanied with a decrease of the hydroxide concentration, and it is the change in hydroxide concentration that is responsible for the potential shift rather than the changes in the carbonate concentration itself, see below. The carbonate levels in electrolyte E4 and E5, would cause a second plateau in the discharge curve for a pocket plate electrode where the hydroxide ions do not have enough time to diffuse into the pores, but in the voltammetry there is only a small positive shift in oxidation potential. The concentration change from E3 to E5 results in a potential shift of about 30 mV, Fig. 5. This small shift of the oxidation peak can not explain the second voltage plateau for the pocket plate electrode. However, in a porous electrode the hydroxide concentration within the porous structure can be much lower than in the bulk. During discharge cadmium is oxidised to cadmium hydroxide which implies the consumption of hydroxide ions. This does not affect the bulk concentration, but within the pores there may be a depletion of hydroxide ions. This makes it interesting to study the pH-dependence of the process.

In order to study the pH dependence at pH levels that can appear in the pores during charge/discharge, cyclic voltammograms of the negative active material in CPEE were run at five different hydroxide ion concentrations which refers to pH 14, 13, 12, 11 and 10, Section 2.2. At pH 14 and 13 solutions of 1 and 0.1 M KOH were used. At lower pH a supporting electrolyte had to be added to avoid resistance effects in the measurements. The carbonate system was chosen as the supporting electrolyte since it is present in the battery. CO_3^{2-} and HCO_3^- are added to decarbonated water in certain ratios to achieve the required hydroxide concentrations. The ratios are calculated from pK_a.

A new CPEE with active material was used at each pH and the electrode was first cycled until a constant response was obtained (4–6 cycles). The scan rate was 1 mV/s. Earlier fundamental studies of the cadmium electrode [3] have shown that there is no rotation dependence of the cadmium oxidation in 1 M alkaline solution, implying that the kinetics are rate determining.

Mechanistic analysis gives a Tafel slope of 31 mV/decade ± 3 mV at all pHs, Eq. (3), which can be interpreted as a one plus one fast electron transfer and the rate determining step is a subsequent chemical step. The potential shift with respect to pH was measured at the same current in

all concentrations, Fig. 5. There were different potential shifts in different pH regions, Eqs. (4) and (5).

$$\frac{\partial E}{\partial \log I} = 33\,\text{mV} \tag{3}$$

$$\left(\frac{\partial E}{\partial \log[\text{OH}^-]}\right)_I = 17\,\text{mV}, \quad \text{for pH 10–12} \tag{4}$$

$$\left(\frac{\partial E}{\partial \log[\text{OH}^-]}\right)_I = 63\,\text{mV}, \quad \text{for pH 12–14} \tag{5}$$

$$\left(\frac{\partial \log I}{\partial \log[\text{OH}^-]}\right)_E = 0.5, \quad \text{for pH 10–12} \tag{6}$$

$$\left(\frac{\partial \log I}{\partial \log[\text{OH}^-]}\right)_E = 2, \quad \text{for pH 12–14} \tag{7}$$

Between pH 10 and 12 the reaction order is 0.5, Eq. (6), and the products in the rate-determining step contain equal parts of Cd^{2+} and $CdOH^+$. This is consistent with the hydrolysis of cadmium at pH 10 [29]. For pH > 10 further hydrolysis of the products in the rate determining step takes place in the bulk solution. For pH between 12 and 14, the reaction order is 2, Eq. (7), such that for each cadmium oxidised, two hydroxide ions are consumed and the product in the rate determining step is consequently $Cd(OH)_2$. Further hydrolysis proceeds out in the bulk solution since the main hydrolysis product at those pH is $Cd(OH)_4^{2-}$ [29]. As expected, the potential for the oxidation of cadmium is shifted in the anodic direction as the OH^- concentration is decreased, Fig. 5. At hydroxide concentrations > 1 M it is not possible to do kinetic analysis since there is mixed kinetic and mass transport control. Anyhow, the same pH dependence as in the concentration range of 0.01–1 M was achieved for hydroxide concentrations > 1 M. The main hydrolysis product of Cd^{2+} at hydroxide concentrations above 1 M is $Cd(OH)_4^{2-}$ [29]. This demonstrates that the oxidised species leaves the surface as $Cd(OH)_2$ (aq) and that the hydrolysis proceeds in the bulk solution.

For a porous structure of the electrode this leads to a mass transport limitation of hydroxide ions, which entails a pH decrease within the pores. In Fig. 5 it can be seen that if the pH is decreased to pH 10 within the porous there will be a shift in positive direction of about 200 mV. This shift is of the same magnitude as the potential shift of the second discharge plateau.

The results from this investigation indicate that the second plateau observed at cadmium pocket plate electrodes is due to an inhomogeneous distribution of hydroxide ions in the negative material during discharging. The cadmium metal formed in the charging (reduction) process is discharged (oxidised) to the hydroxide with consumption of hydroxide ions. In the porous electrode structure the hydroxide ions in the pores may be more or less completely consumed during the charging process. If the diffusion of hydroxide ions from the bulk solution is slow, the pH will be lowered in the pores of the active material, which changes the oxidation potential of cadmium in a positive direction.

The surface analyses, Section 3.3, show that only minor amounts of cadmium carbonate can be detected in the discharged mass, which supports the fact that a pH change rather than cadmium carbonate is the cause of the second discharge plateau. Thus, the second plateau can be explained by the steady state oxidation of cadmium involving slow diffusion of hydroxide ions from the bulk solution and dissolution of cadmium hydroxide, Eqs. (8) and (9), where q can have the values 0, 1 or 2.

$$\text{Cd(s)} + 2\text{OH}^- \underset{\text{reduction/charging}}{\overset{\text{oxidation/discharging}}{\rightleftarrows}} \text{Cd(OH)}_2\text{(s)} + 2\text{e}^- \tag{8}$$

$$\underset{\uparrow}{\text{Cd(OH)}_2\text{(s)} + q\text{OH}^-} \xleftrightarrow{K} \text{Cd(OH)}_{2+q}^{q-}\text{(aq)} \tag{9}$$

Diffusion from the bulk

The scenario for explaining the second plateau would be as follows: cadmium metal is oxidised and hydroxide ions are consumed. If the discharge rate is low and the bulk concentration of hydroxide ions is high (low carbonate concentration) the bulk diffusion can keep up with the consumption of hydroxide ions in the pores and only one discharge plateau is observed. Alternatively, if the discharge rate is high and/or the hydroxide concentration low (high carbonate concentration) there are insufficient hydroxide ions available. This impoverishment of hydroxide ions will result in a shift in the oxidation potential. Hydroxide ions from the bulk will partially dissolve the hydroxide formed on the surface, allowing for a slow continuous oxidation of the underlying cadmium metal. If the hydroxide concentration is too low no further oxidation can take place, resulting in a large capacity loss, as illustrated in Figs. 1b, 2b and 3b.

3.3. X-ray diffraction

The active material was also investigated with the aid of X-ray diffraction in order to analyse the phase composition. Cadmium hydroxide exists in three structures: β-$Cd(OH)_2$, γ-$Cd(OH)_2$ and α-$Cd(OH)_2$. Formation of γ-$Cd(OH)_2$ is favoured at high sodium hydroxide concentrations, whereas β-$Cd(OH)_2$ formation is favoured at high potassium hydroxide concentrations [3,4]. Both hydroxide modifications can exist in a battery but the main phase of the negative electrode is β-$Cd(OH)_2$, which is isostructural with β-$Ni(OH)_2$ having a layer structure and no hydrogen bonds in the crystal [30–34]. The structure of γ-$Cd(OH)_2$ contains a three-dimensional linkage involving weak hydrogen bonds [35]. Earlier investigations of the oxidation behaviour of cadmium forming β-$Cd(OH)_2$ and γ-$Cd(OH)_2$ showed that the oxidation occurs at the same potential independent of which of the product that is formed [3,4]. The initial anodic oxidation product has been suggested to be α-$Cd(OH)_2$,

but no spectroscopic evidence for this phase has been presented [1]. The α-phase is the least stable phase of the hydroxides and it is suggested to convert rapidly into the β-phase.

The X-ray diffraction analysis of the negative active materials from the pocket plate charge/discharge cycling shows that the main phase is β-$Cd(OH)_2$ in the discharged state. No evidence of γ-$Cd(OH)_2$ was found, which was expected since the electrolyte contains KOH and LiOH [4].

The existence of $CdCO_3$ was also examined since it has been reported earlier to be the oxidation product of cadmium in carbonate containing electrolyte [22,23] and that cells with high carbonate concentration exhibit a capacity loss [21,24]. However, only trace amounts of $CdCO_3$ were detected in sample B1 that exhibited the highest carbonate concentration in the electrolyte. No $CdCO_3$ was found in A1, A2 and B2 (electrolyte exchanged). The carbonate content in the electrode from cell B1 was too low to be responsible for the second discharge plateau in the cell.

4. Conclusions

- The origin of a second voltage plateau is related to the discharge rate and to the carbonate concentration in the electrolyte. High discharge rates and high carbonate concentration favour plateau formation, which may result in a capacity loss.
- The second voltage plateau disappears after electrolyte exchanges as a result of increased hydroxide concentration and/or decreased carbonate concentration.
- If the consumption of hydroxide ions caused by the discharge reaction is higher than the hydroxide diffusion from the bulk solution, the hydroxide concentration in the pores is decreasing and the discharge potential shifts in positive direction, resulting in a second voltage plateau.
- Voltammetric measurements have shown that the presence of $CdCO_3$ in the discharged negative electrode can not give rise to a second voltage plateau or capacity loss.
- Only trace amounts of $CdCO_3$ are observed in XRD.

Acknowledgements

We are grateful to the people at SAFT laboratory for performing electrical tests and chemical analyses.

References

[1] Y. Duhirel, B. Beden, J.M. Léger, C. Lamy, Electrochim. Acta 37 (1992) 665.
[2] S.B. Saidman, J.R. Vilche, A.J. Arvia, Electrochim. Acta 32 (1987) 395.
[3] N. Simic, E. Ahlberg, J. Electroanal. Chem. 451 (1998) 237.
[4] N. Simic, E. Ahlberg, J. Electroanal. Chem. 462 (1999) 34.
[5] J.I.D. Urraza, C.A. Gervasi, S.B. Saidman, J.R. Vilche, J. Appl. Electrochem. 23 (1993) 1207.
[6] J.O. Zerbino, S.B. Saidman, J.R. Vilche, A.J. Arvia, Electrochim. Acta 35 (1990) 605.
[7] R. Barnard, K. Edmondson, J.A. Lee, F.L. Tye, J. Appl. Electrochem. 6 (1976) 107.
[8] R. Barnard, K. Edmondson, J.A. Lee, F.L. Tye, J. Appl. Electrochem. 6 (1976) 431.
[9] S. Sathyanarayana, in: J. Thompson (Ed.), Power Sources, Vol. 7, Academic Press, Brighton, 1979, p. 141.
[10] S. Sathyanarayana, J. Appl. Electrochem. 15 (1985) 453.
[11] S. Petrovic, J. Garche, K. Wiesener, J. Mrha, J. Jindra, J. Power Sources 19 (1987) 55.
[12] M.Z.A. Munshi, A.C.C. Tseung, D. Misale, J. Power Sources 23 (1988) 341.
[13] Y. Yamamoto, Electrochim. Acta 36 (1991) 1433.
[14] S.T. Selvam, S.N. Begum, V.R. Chidambaram, R. Sabapathi, K.I. Vasu, J. Power Sources 32 (1990) 55.
[15] R.D. Armstrong, K. Edmondson, J. Electroanal. Chem. 53 (1974) 371.
[16] D. Berndt, Maintenance-free Batteries: Lead-acid, Nickel Cadmium, Research Studies Press Ltd., John Wiley & Sons Inc., Tannton, UK, 1993.
[17] S. Gross, in: Proceedings of NiCad-94, International Cadmium Association, Geneva, Italy, 1994, p. 1.
[18] R. Barnard, J. Appl. Electrochem. 11 (1981) 217.
[19] F.G. Will, H.J. Hess, J. Electrochem. Soc. 120 (1973) 1.
[20] Y.I. Ob'edkov, L.A. L'vova, Élektrokhimiya 9 (1973) 1649.
[21] D.L. Barney, Nickel–Cadmium Battery Application Engineering Handbook, General Electric Co., Gairsville, USA, 1971.
[22] K. Huber, J. Electrochem. Soc. 100 (1953) 376.
[23] E.J. Casey, A.R. Dubois, P.E. Lake, W.J. Moroz, J. Electrochem. Soc. 112 (1965) 371.
[24] S.U. Falk, A.J. Salkind, Alkaline Storage Batteries, Wiley, New York, 1969.
[25] E. Ahlberg, U. Palmqvist, N. Simic, R. Sjövall, J. Power Sources 85 (2000) 245.
[26] C.D.S. Tuck, Modern Battery Technology, Ellis Horwood, Chichester, UK, 1991.
[27] R. Barnard, G.T. Crickmore, J.A. Lee, F.L. Tye, in: D.H. Collins (Ed.), Power Sources, Vol. 6, Academic Press, Brighton, 1977, p. 161.
[28] J. Kankare, Anal. Chem. 44 (1972) 2376.
[29] C.F. Baes, R.E. Mesmer, The Hydrolysis of Cations, Krieger Publishing Company, 1976.
[30] O.K. Srivastava, E.A. Secco, Can. J. Chem. 45 (1967) 3203.
[31] G. Bertrand, Y. Dusausoy, C. R. Acad. Sci. Paris-serie C 270 (1970) 612.
[32] H.D. Lutz, H. Möller, M. Schmidt, J. Mol. Struct. 328 (1994) 121.
[33] B. Weckler, H.D. Lutz, Spectrochim Acta A 52 (1996) 1507.
[34] O. Glemser, U. Hauschild, H. Richert, Z. Anorg. Allg. Chemie. 290 (1957) 58.
[35] A. Riou, Y. Cudennec, Y. Gerault, Mat. Res. Bull. 25 (1990) 987.